



Optimization studies of HgSe thin film deposition by electrochemical atomic layer epitaxy (EC-ALE)

Venkatram Venkatasamy^a, Mkhulu K. Mathe^a, Stephen M. Cox^b,
Uwe Happek^b, John L. Stickney^{a,*}

^a Department of Chemistry, University of Georgia, Athens, GA, United States

^b Department of Astronomy and Physics, Athens, GA, United States

Received 10 October 2005; received in revised form 9 December 2005; accepted 10 December 2005

Abstract

Studies of the optimization of HgSe thin film deposition using electrochemical atomic layer epitaxy (EC-ALE) are reported. Cyclic voltammetry was used to obtain approximate deposition potentials for each element. These potentials were then coupled with their respective solutions to deposit atomic layers of the elements, in a cycle. The cycle, used with an automated flow deposition system, was then repeated to form thin films, the number of cycles performed determining the thickness of the deposit. In the formation of HgSe, the effect of Hg and Se deposition potentials, and a Se stripping potential, were adjusted to optimize the deposition program. Electron probe microanalysis (EPMA) of 100 cycle deposits, grown using the optimized program, showed a Se/Hg ratio of 1.08. Ellipsometric measurements of the deposit indicated a thickness of 19 nm, where 35 nm was expected. X-ray diffraction displayed a pattern consistent with the formation of a zinc blende structure, with a strong (1 1 1) preferred orientation. Glancing angle fourier transform infrared spectroscopy (FTIR) absorption measurements of the deposit suggested a negative gap of 0.60 eV. © 2005 Published by Elsevier Ltd.

PACS: 81.05. D; 81.05. B, C, D, E, G; 81.15. P; 82.45. Q; 61.10. N; 78.66. H

Keywords: B1. HgSe; A3. EC-ALE; A3. UPD; A3. Electrodeposition; A1. XRD; A1. EPMA; A1. FTIR; A3 ALE; A3 ALD

1. Introduction

Mercury selenide, HgSe, is a II–VI compound semiconductor. Based on its electrical properties, it is classified as a semimetal or degenerate semiconductor [1–3]. It is of special interest for fundamental studies because of its inverted band structure [4]. Some of the possible applications for mercury selenide lie in optoelectronics. Molecular beam epitaxy (MBE) [5,6], chemical bath deposition [7–9] and the cold traveling heater method (CTHM) [10] are some of the methods previously used to deposit HgSe.

Recently, this group reported the first deposits of mercury selenide formed via electrochemical atomic layer epitaxy (EC-ALE) [11]. EC-ALE is the electrochemical analog of atomic layer epitaxy (ALE) [12–17], and atomic layer deposition (ALD) [18–21]. All are methods for which the deposits are grown

layer by layer, using surface limited reactions, under potential deposition (UPD) in the case of EC-ALE. UPD refers to the electrodeposition of an atomic layer of a first element on a second, at a potential prior to, under, that needed to deposit the element on itself [22–26]. A number of II–VI compounds such as CdTe, CdS and ZnSe have been successfully grown using EC-ALE [27–30], as well as some III–V compounds such as GaAs, InAs and InSb [28,29,31,32]. Recently PbSe [33], PbTe and Bi₂Te₃ [34] have also been grown using EC-ALE.

This paper is an extension of previous work on HgSe deposition by this group [11]. Attempts have been made to optimize the deposition cycle of HgSe, by adjusting the potentials for Se and Hg used in the EC-ALE cycle.

2. Experimental

Depositions were performed using a thin layer flow electrodeposition system [16,35,36], which consisted of pumps, valves, a flow cell and a potentiostat. All components were computer controlled using a LABVIEW program.

* Corresponding author. Tel.: +1 706 542 2726; fax: +1 706 542 9454.
E-mail address: stickney@chem.uga.edu (J.L. Stickney).

The flow cell has been previously described [37], with minor design changes to the reference compartment. A Teflon tube fitting was changed to a simple O-ring, which provided a better seal. The auxiliary electrode was an ITO glass slide, and the reference electrode was Ag/AgCl (3 M NaCl) (Bioanalytical Systems Inc., West Lafayette, IN). Substrates consisted of 300 nm thick gold films on glass. The substrates were annealed at 400 °C for 12 h under a vacuum of 10^{-6} Torr, after Au vapor deposition, resulting in a (1 1 1) habit.

The solutions used were 0.2 mM HgO, pH 2 and 0.5 mM SeO₂, pH 3. Both solutions contained 0.5 M Na₂SO₄ as a supporting electrolyte. The blank solution contained only the 0.5 M Na₂SO₄, at pH 4. Solution pH was adjusted using H₂SO₄. The water used to make solutions was supplied from a Nanopure water filtration system (Barnstead, Dubuque, IA) attached to the house DI water system. Chemicals were reagent grade or better.

The EC-ALE cycle used to deposit HgSe was performed as follows: the Se solution was flushed into the cell for 2 s (40 mL/min), and then held quiescent for 15 s, all at the chosen Se deposition potential. Blank solution was then flushed through the cell for 3 s. This was followed by filling the cell with the Hg solution for 2 s, and holding quiescent for 15 s for deposition. The cycle was then completed by flushing with blank solution for 3 s. This cycle was repeated 100 times for each experiment.

Deposit thickness was monitored using a single wavelength ellipsometer (Sentech SE 400). A Scintag, PAD-V diffractometer with Cu K α radiation ($\lambda = 1.5418$ Å), was used to obtain the glancing angle X-ray diffraction patterns. Electron probe Microanalysis (EPMA) was run on a Joel 8600 wavelength dispersive scanning electron microprobe.

Glancing angle absorption measurements were performed, using an FTIR spectrophotometer (Bruker FTS-66v, Bruker optics Inc.).

3. Results and discussions

Cyclic voltammetry was used to determine approximate starting deposition potentials for the EC-ALE cycle. The voltammetric behaviors of HSeO₃⁻ and Hg²⁺ with gold on glass substrates are shown in Figs. 1 and 2. Potentials of 0.20 V for Se and 0.45 V for Hg were identified as reasonable initial potentials for the EC-ALE cycle. Thus, the initial program went as follows: the cell was filled with the Se solution, pumped for 2 s at 0.20 V, no flow (static) for 15 s for deposition, then blank solution was flushed for 3 s at 0.2 V. The Hg solution flush in, pumped for 2 s at 0.45 V, static for 15 s, and blank solution flush for 3 s at 0.45 V. The intent was that this cycle would ideally result in the deposition of one compound monolayer.

Using these conditions, no deposition was observed by visual inspection after 100 cycles. Evidently the potentials chosen were insufficiently negative to drive the deposition of HgSe, even though UPD of these elements on Au looked promising. This points out that the potentials derived from voltammetry on the substrate are simply a good first approximation for the potentials needed for a cycle, but do not represent the potentials needed to deposit the elements on each other.

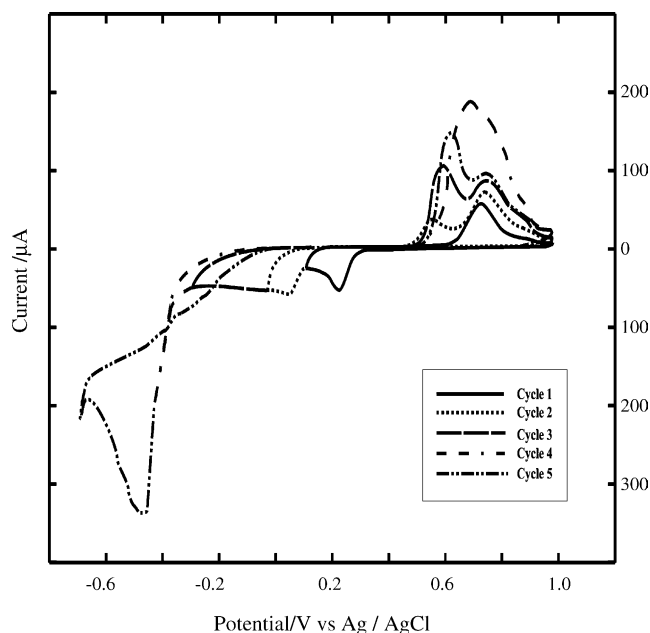


Fig. 1. Cyclic voltammogram of Au electrode in 0.5 mM HSeO₃⁻, pH 3 (electrode area: 4 cm²; scan rate: 5 mV/s).

A series of experiments were then performed where the deposition potentials for Se were varied from 0.20 to -0.20 V, while keeping the same deposition potential for Hg at 0.45 V (Fig. 3). No deposits were evident until the potential for Se deposition was -0.10 V or below. Optical microscopy and EPMA were performed on each deposit to determine homogeneity and stoichiometry, respectively. Based on deposit homogeneity, -0.15 V was selected as a good Se deposition potential. The resulting deposits appeared homogeneous and stoichiometric, however, ellipsometric data suggested the deposits were close

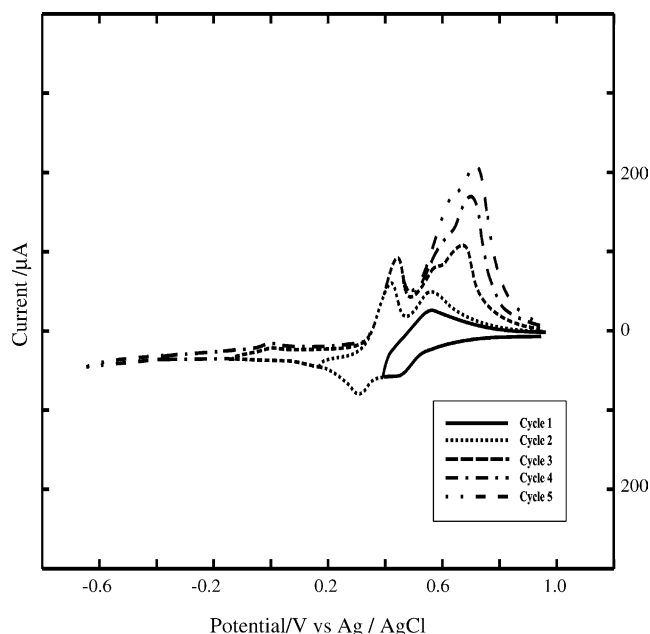


Fig. 2. Cyclic voltammogram of Au electrode in 0.2 mM Hg²⁺, pH 2 (electrode area: 4 cm²; scan rate: 5 mV/s).

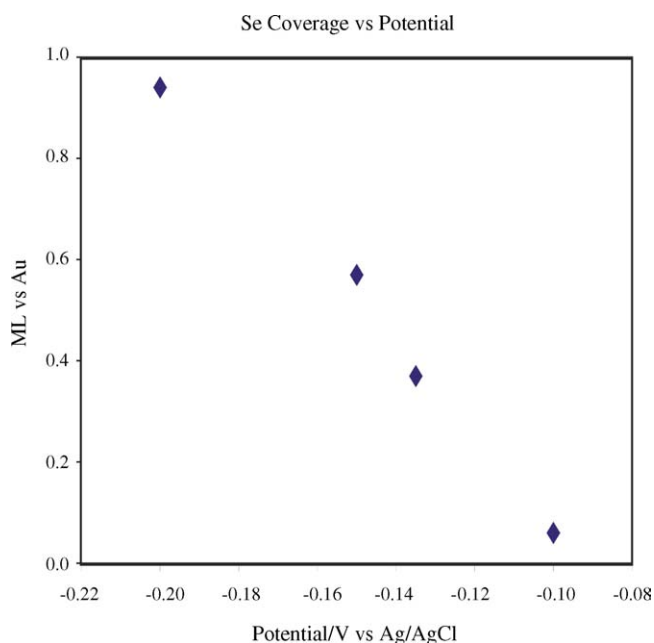


Fig. 3. Effect of Se deposition potential on HgSe deposition (Hg deposition potential: 0.48 V; Se stripping potential: -0.63 V).

to 100 nm thick, significantly thicker than expected for a simple model of one compound monolayer per cycle, where a 100 cycle deposit was expected to result in a 37.4 nm thick film. This model assumes one Hg–Se bi-layer grows each cycle, with the (1 1 1) orientation [37].

Previous studies of Se deposition [38,39] have shown that Se does not result in a classic underpotential deposition process. On the contrary, Se deposition requires an over potential, but bulk deposition of Se is so slow that a surface limited feature is still visible. The result is that along with the surface limited reaction, formation of an atomic layer of Se, a small amount of bulk Se is deposited as well. This can be seen from the current time profile, during Se deposition (Fig. 4). The current for Se deposition does not drop down to zero after the surface is covered, that suggests that it is not a surface limited process and the amount of bulk Se deposited depends on the deposition time. The surface limited process is fast, reaching completion quickly, while the

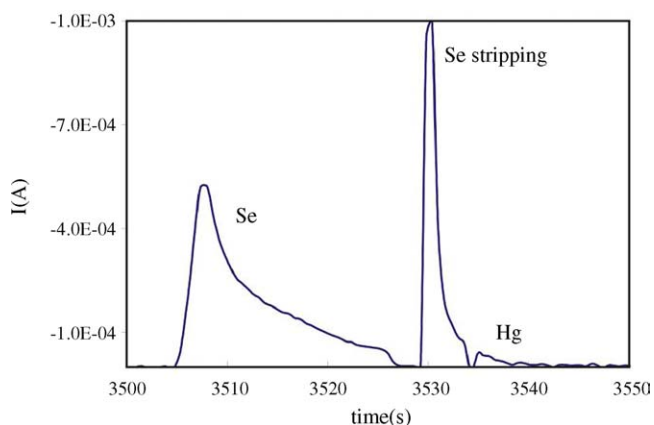


Fig. 4. Current–time profile during one cycle of HgSe deposition using ideal deposition program.

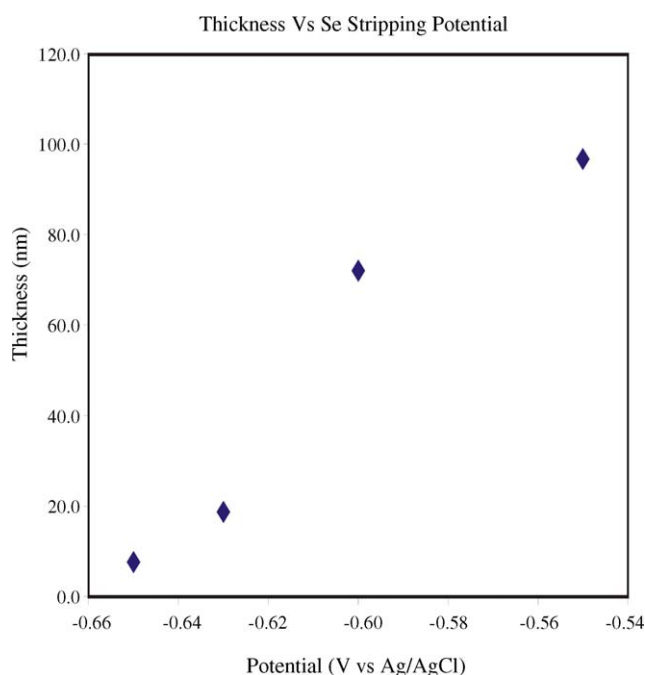


Fig. 5. Effect of Se stripping potential on deposit thickness.

bulk deposition is slow, resulting in a small steady state current [40]. Thus, one explanation for the excess deposit thicknesses is the formation of some bulk Se on the surface. Deposition of bulk Se can be minimized by using a short deposition time, just long enough for the majority of the surface limited deposition to complete. Alternatively, bulk Se can be removed by introduction of an extra step designed to reduce excess bulk Se to a soluble selenide species [27]. This second methodology was selected for the present study. After 15 s of Se deposition, the cell was rinsed with blank solution for 3 s, at which point the potential was shifted negatively, such that bulk Se was reduced to HSe^- . HSe^- is a soluble species, which diffuses away, leaving only up Se on the surface. A set of experiments were performed by varying this reductive stripping potential for Se from -0.55 to -0.65 V, while keeping all the other parameters constant (Fig. 5). Based on the resulting deposit stoichiometry data from EPMA, and optical microscopy observations of the deposit thickness and homogeneity, -0.63 V was picked as the reductive stripping potential for the cycle.

To optimize the deposition potential for Hg, another series of experiments were conducted, where only the deposition potential for Hg (Fig. 6) was varied. The best Hg deposition potential appeared to be 0.48 V, based on stoichiometry and optical microscopy. However, it is of note that the coulometry for Hg, at this potential, suggested a coverage of only 0.10 ML^1 , instead of the 0.44 ML ideally expected. Previous results have suggested that the formation of one bi-layer of Cd and Se from the (1 1 1) plane of zinc blende CdSe would require 0.44 ML of Cd and 0.44 ML of Se. It is not clear why the coulometry for Hg was so

¹ Coverages used in this paper are relative to the number of Au surface atoms. Hence, 1 ML here would refer to one deposited metal atom for each Au surface atom.

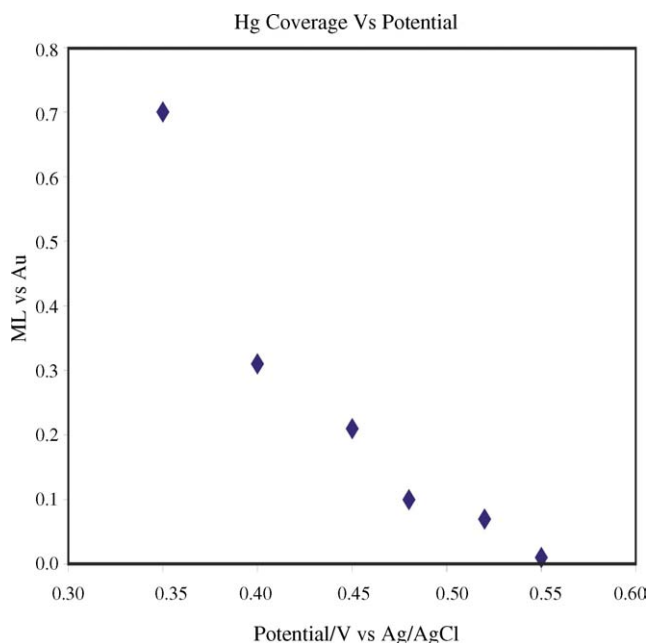


Fig. 6. Effect of Hg deposition potential on HgSe deposition (Se deposition potential: -0.15 V; Se stripping potential: -0.63 V).

low, 0.10 ML versus 0.44 ML. One possibility is that some of the deposited Se was oxidized at the positive potentials required for surface limited Hg deposition. The coulometry observed was thus the net charge for Hg^{2+} reduction and Se oxidation. In addition, the resulting films were about half as thick as ideally expected, where deposition of a compound monolayer is expected with each cycle, see below.

Overall, the optimal EC-ALE cycle for HgSe deposition appeared to be as follows: Se solution was rinsed into the cell

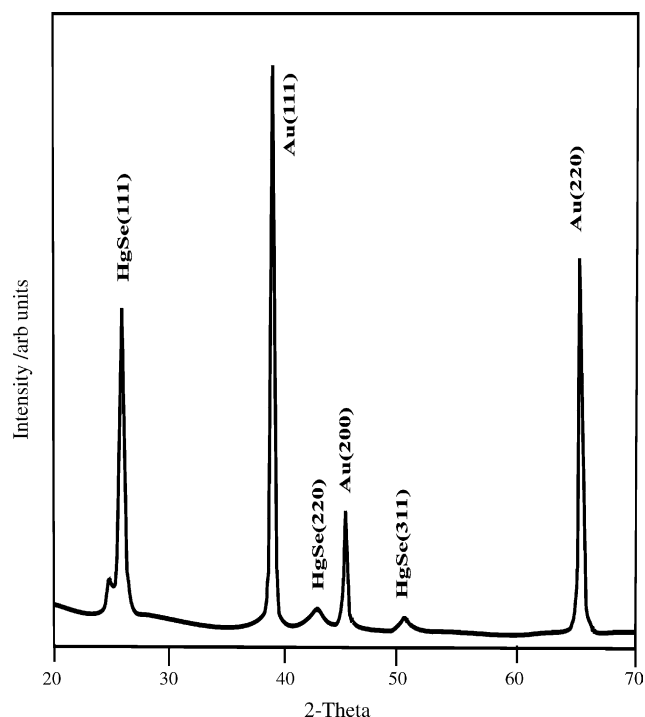


Fig. 8. XRD diffraction pattern of 100 cycle HgSe thin film.

for 2 s at -0.15 V. The solution was held static for 15 s for deposition. The cell was then flushed with blank solution for 3 s at -0.15 V, at which point, the potential was changed to -0.63 V for 5 s. After this, the Hg solution was filled for 2 s, and deposited for 15 s at 0.48 V. This was followed by another blank rinse at 0.48 V for 3 s (Fig. 7).

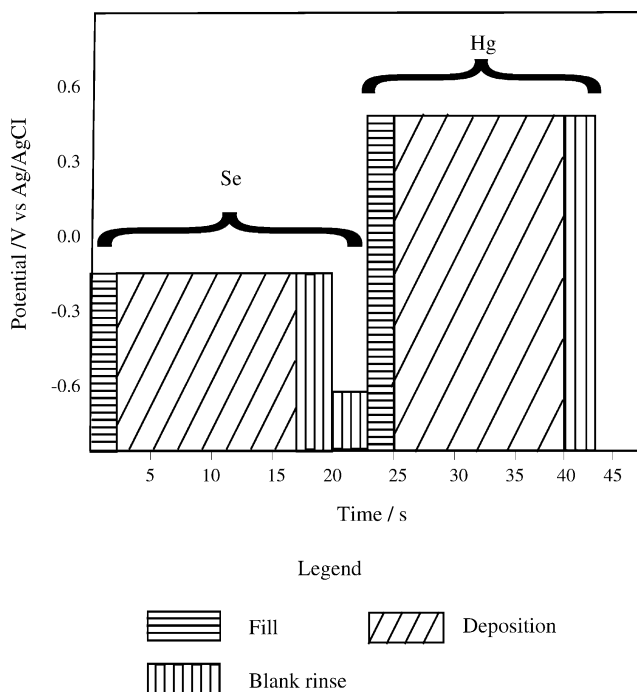


Fig. 7. Optimal deposition program.

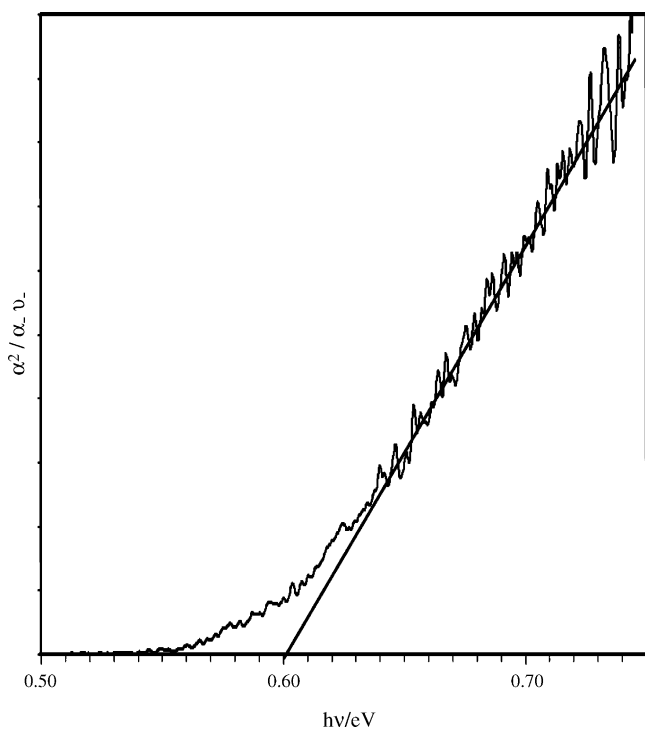


Fig. 9. Absorption spectrum of 100 cycles HgSe thin film.

Ellipsometric measurements of the resulting deposit indicated that the film was 19 nm thick. EPMA of the deposit indicated a Se/Hg atomic ratio of 1.08. Fig. 8 shows the X-ray diffraction pattern for the deposit. Peaks corresponding to (1 1 1), (2 2 0) and (3 1 1) planes of HgSe (JCPDS 8-469) were evident, and no elemental peaks for Hg and Se were observed. The deposit showed a predominant (1 1 1) orientation as the ratio of the intensity between the (1 1 1) and (2 2 0) peak came out to be 10.2, which is considerably higher than the literature value of 2.

Room temperature IR absorption studies of HgSe were performed using a glancing angle of 85° from the surface normal. Fig. 9 shows a plot of the square of the absorption data versus energy for a 100-cycle deposit of HgSe. An absorption edge was found at -0.60 eV. This value corresponds to the $\Gamma_6^{VB} \rightarrow \Gamma_8^{CB}$ transition of the inverted band structure of HgSe, reported to be -0.51 eV from theoretical calculations [41] and -0.46 eV experimentally [4].

4. Conclusion

The influence of the deposition potentials for Hg and Se, as well as that for a reductive Se stripping step, has been reported. The optimal deposition cycle devised includes deposition of Se at -0.15 V, stripping of excess Se at -0.63 V, and deposition of Hg at 0.48 V. The resulting deposit was a little over half of that expected from the ideal model of one compound monolayer for each cycle, but the deposit was stoichiometric, and showed strong preferential (1 1 1) deposition. The absorption spectrum for this deposit appears consistent with the literature: an inverted band structure and a negative gap of 0.6 eV.

Acknowledgements

The authors would like to acknowledge the support of NSF divisions of Chemistry and Material science.

References

- [1] T.C. Harman, A.J. Strauss, *J. Appl. Phys.* 32 (1961) 2265.
- [2] P.W. Kurse, M.D. Blue, *J. Phys. Chem. Solids* 23 (1963) 577.
- [3] K.U. Gawlik, L. Kipp, M. Skibowski, N. Orłowski, R. Manzke, *Phys. Rev. Lett.* 78 (1997) 3165.
- [4] S. Einfeldt, F. Goschenhofer, C.R. Becker, G. Landwehr, *Phys. Rev. B* 51 (1995) 4915.
- [5] S. Einfeldt, H. Heinke, M. Behringer, C.R. Becker, E. Kurtz, D. Hommel, G. Landwehr, *J. Cryst. Growth* 138 (1994) 471.
- [6] C.R. Becker, L. He, S. Einfeldt, Y.S. Wu, G. Lerondel, H. Heinke, S. Oehling, R.N. Bicknell-Tassius, G. Landwehr, *J. Cryst. Growth* 127 (1993) 331.
- [7] P.P. Hankare, V.M. Bhuse, K.M. Garadkar, A.D. Jadhav, *Mater. Chem. Phys.* 71 (2001) 53.
- [8] P. Pramanik, S. Bhattacharya, *Mater. Res. Bull.* 24 (1989) 945.
- [9] Y. Li, Y. Ding, H. Liao, Y. Qian, *J. Phys. Chem. Solids* 60 (1999) 965.
- [10] C. Reig, Y.S. Paranchych, V. Munoz-Sanjose, *Cryst. Growth Design* 2 (2002) 91.
- [11] S.M. Cox, M.K. Mathe, V. Venkatasamy, U. Happek, J.L. Stickney, *J. Electrochem. Soc.* 152 (2005) C751.
- [12] S. Bedair, *Atomic Layer Epitaxy*, Elsevier, Amsterdam, 1993.
- [13] T.F. Kuech, P.D. Dapkus, Y. Aoyagi, *Atomic Layer Growth and Processing*, Materials Research Society, Pittsburgh, 1991.
- [14] H.L. Colin, Goodman, M.V. Pessa, *J. Appl. Phys.* 60 (1986) R65.
- [15] W. Faschinger, *Phys. Scr.* T49B (1993) 492.
- [16] J.L. Stickney, *Electroanalytical Chemistry*, vol. 21, Marcel Dekker, New York, 1999, p. 75.
- [17] B.W. Gregory, J.L. Stickney, *J. Electroanal. Chem.* 300 (1991) 543.
- [18] M. Leskela, M. Ritala, *Thin Solid Films* 409 (2002) 138.
- [19] E.B. Yousfi, B. Weinberger, F. Donsanti, P. Cowache, D. Lincot, *Thin Solid Films* 387 (2001) 29.
- [20] V. Sammelselg, A. Rosental, A. Tarre, L. Niinisto, K. Heiskanen, K. Ilmonen, L.-S. Johansson, T. Uustare, *Appl. Surf. Sci.* 134 (1998) 78.
- [21] M. Ylilammi, *Thin Solid Films* 279 (1996) 124.
- [22] D.M. Kolb, M. Przasnys, H. Gerische, *J. Electroanal. Chem.* 54 (1974) 25.
- [23] D.M. Kolb, *Advances in Electrochemistry and Electrochemical Engineering*, vol. 11, John Wiley, New York, 1978, p. 125.
- [24] K. Juttner, W.J. Lorenz, *Z. Phys. Chem. N. F.* 122 (1980) 163.
- [25] A.T. Hubbard, V.K.F. Chia, D.G. Frank, J.Y. Katekaru, S.D. Rosasco, G.N. Salaita, B.C. Schardt, D. Song, M.P. Soriaga, *New Dimensions in Chemical Analysis*, Texas A&M University Press, College Station, TX, 1985, p. 135.
- [26] A.A. Gewirth, B.K. Niece, *Chem. Rev.* 97 (1997) 1129.
- [27] L.P. Colletti, B.H. Flowers Jr., J.L. Stickney, *J. Electrochem. Soc.* 145 (1998) 1442.
- [28] T.L. Wade, B.H. Flowers Jr., U. Happek, J.L. Stickney, Presented at the National Meeting of the Electrochemical Society, Spring, Seattle, Washington, 1999.
- [29] T.L. Wade, B.H. Flowers Jr., R. Vaidyanathan, M.K. Mathe, C.B. Maddox, U. Happek, J.L. Stickney, Presented at the Materials Research Society, 2000.
- [30] J.L. Stickney, K. Varazo, L.C. Ward, M.D. Lay, T. Sorenson, *Encyclopedia of Surface and Colloid Science*, Marcel Dekker Inc., New York, 2002.
- [31] T.L. Wade, L.C. Ward, C.B. Maddox, U. Happek, J.L. Stickney, *Electrochem. Solid State Lett.* 2 (1999) 616.
- [32] T.L. Wade, R. Vaidyanathan, U. Happek, J.L. Stickney, *J. Electroanal. Chem.* 500 (2001) 322.
- [33] R. Vaidyanathan, J.L. Stickney, U. Happek, *Electrochim. Acta* 49 (2004) 1321.
- [34] J.Y. Yang, W. Zhu, T.J. Zhang, *Electrochim. Acta* 50 (2005) 4041.
- [35] T.L. Wade, T. Sorenson, J.L. Stickney, *Interfacial Electrochemistry*, Marcel Dekker, New York, 1999, p. 757.
- [36] T.L. Wade, B.H. Flowers Jr., K. Varazo, M. Lay, U. Happek, J.L. Stickney, Presented at the Electrochemical Society National Meeting, Washington, D.C., 2001.
- [37] B.H. Flowers Jr., T.L. Wade, J.W. Garvey, M. Lay, U. Happek, J.L. Stickney, *J. Electroanal. Chem.* 524 (2002) 273.
- [38] B.M. Huang, T.E. Lister, J.L. Stickney, *Surf. Sci.* 392 (1997) 27.
- [39] N.N. Greenwood, A. Earnshaw, *Chemistry of the Elements*, Pergamon Press, Oxford, 1984.
- [40] T.E. Lister, J.L. Stickney, *Appl. Surf. Sci.* 107 (1996) 153.
- [41] M. Rohlfing, S.G. Louie, *Phys. Rev. B* 57 (1998) R9392.